M R S Internet Journal Nitride Semiconductor Research

Photoluminescence in n-doped $In_{0.1}Ga_{0.9}N/In_{0.01}Ga_{0.99}N$ multiple quantum wells

B. Monemar[1], P.P.Paskov[1], J. P. Bergman[1], G. Pozina[1], V. Darakchieva[1], M. Iwaya[23], Satoshi Kamiyama[23], H. Amano[23] and I. Akasaki[23]
[1]*Department of Physics and Measurement Technology, Linköping University,*
[2]*Department of Electrical and Electronic Engineering, Meijo University,*
[3]*High-Tech Research Center, Meijo University,*

(Received Tuesday, August 27, 2002; accepted Monday, October 7, 2002)

$In_{0.1}Ga_{0.9}N/In_{0.01}Ga_{0.99}N$ multiple quantum wells (MQWs) with heavily Si-doped barriers, grown with Metal Organic Vapor Phase Epitaxy (MOVPE) at about 800^0C, have been studied in detail with optical spectroscopy. Such structures are shown to be very sensitive to a near surface depletion field, and if no additional layer is grown on top of the MQW structure the optical spectra from the individual QWs are expected to be drastically different. For a sample with 3 near surface QWs and Si-doped barriers, only the QW most distant from the surface is observed in photoluminescence (PL). The strong surface depletion field is suggested to explain these results, so that the QWs closer to the surface cannot hold the photo-excited carriers. A similar effect of the strong depletion field is found in an LED structure where the MQW is positioned at the highly doped n-side of the pn-junction. The internal polarization induced electric field in the QWs is also rather strong, and incompletely screened by carriers transferred from the doped barriers. The observed PL emission for this QW is of localized exciton character, consistent with the temperature dependence of peak position and PL decay time. The excitonic lineshape of 35-40 meV in the QW PL is explained as caused by a combination of random alloy fluctuations and interface roughness; the corresponding localization potentials are also responsible for the localization of the excitons in the low temperature range (<150 K). These samples show no evidence of localization due to nanoscale In fluctuations, these commonly observed problems are concluded to be not present in our samples. A second PL feature at lower energy, observed at low temperatures, is shown to be related to an electron pocket at the interface to the underlying n-GaN buffer layer in these samples.

1 Introduction

The $In_xGa_{1-x}N/In_yGa_{1-y}N$ materials system employing quantum wells (QWs) of a thickness about 3 nm is of very high interest for applications in light-emitting diodes (LEDs) and lasers for the visible and near UV spectral regions [1]. There are many investigations of such multiple quantum well (MQW) systems, with different conclusions about the physical origin of the optical emissions from such structures [2] [3] [4] [5] [6] [7]. A very common suggestion is that the main PL emission is due to zero-dimensional nm size features in the QWs, of a higher In content than the main matrix [2] [3] [4] [5] [6] [7] [8]. Evidence from structural investigations for the presence of such quantum dot (QD) like structures in many samples has been presented [9] [10]. Other investigations report the absence of such In-rich inclusions from TEM data [11], indicating that the structure of the well material is very much dependent on the details of the growth conditions employed. It is generally agreed that the low temperature PL spectra of such MQWs are influenced by both localization and the internal polarization induced electric fields [2] [12], but the detailed physics is still under debate. The experimentally derived internal electric fields vary within wide limits, with some authors finding large fields [6], while in most cases the fields are generally much smaller than the theoretical predictions in the case of InGaN/GaN QWs [2] [13] [14]. The reason for the large spread in extracted values for the polarization fields, and the resulting disagreement with the predicted theoretical values [15] [16] [17] [18], is not understood, since for

https://doi.org/10.1557/S1092578300000338 Published online by Cambridge University Press

the AlGaN/GaN MQW system there seems to be a rather good agreement between experimental data and theoretical predictions concerning polarization induced electric fields [14]. The reasons for the observed localization behavior at low temperatures are also not clear, since predictions of localization of holes due to small clusters of In (a few atoms) need to be experimentally confirmed in a broader range of samples [19].

Another problem concerns the interpretation of PL data for nitride MQWs. In the literature it is most often assumed that PL measurements on MQW samples provide average spectral information of the MQW region, so that all quantum wells (QWs) contribute. We will demonstrate that this may in general not be true for this materials system, due to the presence of a large uncompensated polarization charge at the outer surfaces in this wide bandgap system. The resulting near surface depletion potential causes a strong difference in properties for individual QWs in an MQW structure, in particular for highly doped samples with no capping layer on top of the MQW. It was recently demonstrated that in the common case with a highly Si-doped near surface MQW, only one QW appears to contribute to the measured PL signal [20].

2 Samples and experimental procedure

Results for two specific samples are discussed in this paper. Both are grown by Metal Organic Vapor Phase Epitaxy (MOVPE) on a (0001) sapphire substrate with a low temperature AlN buffer layer, followed by a nominally undoped GaN layer [21]. Finally, for sample A, three $In_{0.12}Ga_{0.88}N$ quantum wells of nominal width 3.5 nm were grown on the top of the GaN layer (Figure 1a). The barriers of nominal thickness 10.5 nm were $In_yGa_{1-y}N$ with a small In composition (y = 0.01), doped with Si to about 5×10^{18} cm^{-3}. A second sample, B, had five 3 nm $In_{0.11}Ga_{0.89}N$ QWs separated by 6 nm Si doped $In_{0.01}Ga_{0.99}N$ barriers with a similarly low In content, but had a p-type contact on top, and a semitransparent top metallisation as well (see Figure 1b). The MQW part was grown at a constant growth temperature of about 800°C in both samples. Transmission electron microscopy (TEM) investigations were performed on a large number of such MQW samples grown under similar conditions. The InGaN well material was consistently found to be homogeneous, i. e. no phase separation involving nm-size In rich inclusions in the QWs was observed.

High-resolution X-ray diffraction (HRXRD) and reciprocal space mapping (RSM) were performed using a Philips X'pert MRD triple axis diffractometer. A parabolic graded multilayer mirror collimator, followed by a channel-cut 2-bounce Ge (220) monochromator on the primary side and an asymmetric 2-bounce Ge (220) analyzer crystal giving a resolution of 36 arcsec were used. The RSMs were recorded as consecutive coupled 2θ-ω scans each separated by an ω offset.

For optical excitation in the PL measurements we have used a 266 nm continuous wave (cw) laser. For the transient PL data we used the third harmonics (λ_{exc} = 266 nm) from a Ti:sapphire femtosecond pulse laser. The cw luminescence was detected by a UV enhanced charge coupled detector (CCD). For some experiments a micro-PL setup with a UV objective allowing a spatial resolution of about 1.5 μm was used. The PL transients were detected either by a time-correlated photon counting system with time resolution better than 200 ps, or with a UV sensitive streak camera system. PL excitation (PLE) spectra were obtained with a simple arrangement using a Xe lamp and a monochromator as excitation source. The samples were placed in variable temperature cryostats for measurements at 2 K - 300 K.

3 Structural characterization

Figure 2 shows the experimental diffraction pattern of the 0002 reflection of $In_xGa_{1-x}N/In_yGa_{1-y}N$ MQW sample A. The diffraction profile of the sample was simulated based on the assumption of totally strained InGaN layers, and the best fit to the experiment gives In composition x = 0.12 and y = 0.01 for the well and barrier layers, respectively. The period of the MQW structure was determined to be 11 nm with well thickness of 3 nm and barrier thickness of 8 nm, which are somewhat smaller than the nominal thicknesses.

An asymmetric 10-15 HR-RSM of sample A is shown in Figure 3. Diffraction from the reciprocal space point of the GaN layer and the zero order and the first-satellite associated with the MQW can be seen. The map of the GaN layer is elongated in the lateral direction indicating a mosaic spread typical for III-nitride layers. It is seen from Figure 3 that there is mostly a distribution of diffusely scattered intensity around the MQW satellites, arising from the rough interfaces and possibly resulting from structural defects. The vertical line in Figure 3 marks the location where the reciprocal lattice points of pseudomorphic InGaN MQWs would appear. It clearly shows that the MQW structure is grown coherently on the GaN layer and both the barrier and the well have the same in-plane lattice parameter as the underlying GaN layer. This allows us to use a precise procedure of measuring the GaN in-plane lattice parameter [22] and to adopt it for the InGaN barrier and well layers. We also note that the assumption of totally strained InGaN layers used in the simulation to estimate the In composition is verified.

Measuring a set of symmetric and asymmetric peaks we determined an in-plane lattice parameter of 3.1859 Å

https://doi.org/10.1557/S1092578300000338 Published online by Cambridge University Press

for the thick GaN buffer layer, which shows that the layer is compressively stressed. To determine the in-plane strain in the well and barrier layer we calculated the respective strain-free lattice parameters for the two compositions assuming validity of the Vegard's law. We used the following values: c_{GaN}=5.1851 Å, a_{GaN}=3.1894 Å [22] and c_{InN}=5.7033 Å, a_{InN}=3.5378 Å [23]. Then, having the value of the in-plane strain, the piezoelectric polarizations and the internal electric fields can be calculated [12] [18]. The stiffness, piezoelectric and dielectric constants used in the calculations were obtained by linear interpolation from the binaries [24] [25] [26] [15] [27]. The spontaneous polarization was assumed to have the same value for the well and barrier layers (P_{sp} = –0.029 C/m^2 [15]). The values of the parameters used in the calculations and the resulting piezoelectric polarizations and internal electric fields are summarized in Table 1.

4 Experimental results

4.1 Sample A

4.1.1 Steady-state photoluminescence

The cw PL spectrum at 2 K from the MQW sample A discussed here is shown in Figure 4. The PL linewidth of the main peak Q1 is about 40 meV, depending somewhat on the excitation intensity. We note that there is no obvious dependence of this PL linewidth on the threading dislocation density in these samples, as discussed separately [28]. The PL linewidth of excitons in this MQW system is influenced by both the alloy broadening and the interface roughness, as discussed in more detail below. We interpret the Q1 peak as a localized QW exciton transition, in a QW, which has a certain electron filling due to transfer of donor electrons from the Si doped barriers. The S-shaped temperature dependence of the spectral position confirms this interpretation. In Figures 5a and Figure 5b the temperature dependence of the Q1 PL peak position for two different excitation intensities is shown. The curves are fitted with the standard expression $E = E_0 - \alpha T^2/(T+\beta) - \sigma^2/kT$. For low excitation intensities the σ parameter, representing a measure of the depth of localization potentials, is found to be about 16 meV, at higher excitation intensity a value of 13 meV is found (Figure 5b). This is consistent with expectation, since at higher excitation intensity the deeper localisation potentials are believed to be of less importance in the recombination process. A localization energy for Q1 of about 18 meV is deduced from the Arrhenius plot of the temperature dependence of the integrated PL intensity.

A weaker low energy peak Q2 is observed about 0.1 eV below the main PL peak (Figure 4). This peak is due to a separate PL transition, i. e. not an LO replica of Q1. This is more easily observed when the PL spectra at different excitation intensities are displayed on a log scale (Figure 6). The Q2 transition is increased in strength with increasing excitation intensity at 2 K and shifts to higher energy much faster than the Q1 transition (Figure 7). The upshift of the Q1 peak position is quite small, as expected for the partly screened localization potentials in this case where some electron filling in the QW is expected. With increasing temperature the low energy PL spectrum disappears already at about 20 K at low excitation power (Figure 8a), leaving only the Q1 transition at room temperature (Figure 8b). The emission at T > 20 K consists of the no-phonon Q1 line and successive phonon replicas of 91 meV LO phonons. Note that there is no additional PL emission at photon energies below the near bandgap region, consistent with the absence of localization in nanometer size In-rich regions of the sample. A weak broad peak observed at around 2.2 eV was identified as the so-called yellow luminescence (YL) from the GaN buffer layer, i. e. not related to the MQW region.

The LO phonon coupling strength is rather large, the Huang-Rhys factor S is about 0.3 at low temperature. This is a manifestation of the importance of exciton localization, as discussed separately [29]. At higher temperature the exciton localization is gradually overcome, and the S-value becomes temperature dependent, as expected when free excitons are coming into play [29]. The PL linewidth at 300 K is about 85 meV; the strength of the LO replicas is difficult to measure accurately at this temperature (Figure 8b).

Photoluminescence excitation (PLE) spectra at 2 K are shown in Figure 9. The PLE response for Q1 and Q2 are separately recorded, at low excitation intensity. Clearly the Q1 transition is excited efficiently directly via the QW states, as well as via the $In_yGa_{1-y}N$ barrier with absorption just below the GaN bandgap. The Q2 transition has a very different PLE spectrum. It is not excited efficiently via the QW states, and not via the $In_yGa_{1-y}N$ barriers. Instead it is strongly excited at the GaN bandgap. This is strong evidence for the interpretation of the origin of the Q2 transition as related to an electron potential minimum at the interface to the GaN buffer layer, as shown schematically in Figure 10.

Additional experiments with resonantly excited PL spectra with excitation photon energies close to the QW bandgap show that it is actually possible to excite both transitions in the energy range around Q1 (see Figure 11). This may be interpreted as consistent with the potential suggested in Figure 10, and the fact that only the photo-excited holes in the QW are needed for the Q2 transition to occur. Two-step excitation via defects in GaN may also contribute to the Q2 emission at these

https://doi.org/10.1557/S1092578300000338 Published online by Cambridge University Press

low excitation energies. Note that the spectra in Figure 11 are taken with a ps pulse excitation, which means orders of magnitude higher excitation densities compared to the PLE data in Figure 9. This is presumably the reason why the Q2 peak can be readily excited via Q1 absorption spectrum in Figure 11.

4.1.2 Time-resolved photoluminescence

The PL transients for the Q1 transition exhibit a strongly non-exponential decay behaviour (Figure 12), as expected for this QW system due to the dynamic interplay between the screening of the internal electric field by photo-excited carriers (excitons) and the simultaneous excitation transfer between localization potentials [5]. The initial 1/e decay time is an approximate measure of the radiative QW exciton lifetime at low temperature and varies around 5 ns at 2 K, slightly longer at the low energy wing of the Q1 peak (Figure 12). This is close to the expected radiative lifetime of excitons at 2 K in a 3 nm InGaN/GaN QW [30]. A synopsis of the time-resolved PL spectra at 3 different temperatures is given in Figure 13. At 2 K the presence of the Q2 transition is clearly visible, at 70 K or higher only the Q1 transition is seen, consistent with the cw PL spectra discussed above.

The temperature dependence of the initial decay time for the Q1 transition reveals an approximately constant decay time up to about 150 K and then it drops somewhat due to dominance of nonradiative transitions (Figure 14). The constant decay time at low temperatures is expected due to localization of the excitons in the QW, consistent with the thermal activation energies discussed above. Note that this behaviour is not a proof of the presence of quantum dot localization as argued in many papers, it is just a manifestation of exciton localization in any type of localization potential. In this case we would expect the radiative lifetime of the free excitons to show a linear rise with temperature if they behave as two-dimensional excitons [31]. This behaviour is masked by the localization in the low temperature range, and by nonradiative processes in the high temperature range. We therefore believe the radiative lifetime for the free excitons is simply not observed in these experiments.

4.2 Sample B

4.2.1 Steady-state photoluminescence

The cw PL spectrum of sample B at 2 K is shown in Figure 15. The spectrum shows two peaks, labeled Q1 and Q2, just like for sample A in Figure 4. The PL linewidth of the Q1 peak is narrow, about 35 meV, i. e. similar to the case in sample A. We interpret this peak as due to the lowest QW in the structure, i. e. the one closest to the GaN buffer, similar to the Q1 peak in sample A. The Q2 peak is more complex in this sample, as shown in Figure 16. The dependence on excitation power density is similar to the case in sample A in the sense that the emission increases in intensity more than Q1. In addition it shows a double-peak behaviour at intermediate excitation power. A study of the temperature dependence of this peak reveals a clear double-peak structure at both high and low excitation densities (Figures 17a and 17b). At low excitation power this Q2 structure disappears above 50 K (Figure 17a), while at higher excitation the structure changes at about 70 K, and one of the peaks survives up to temperatures well above 100 K (Figure 17b).

We tentatively explain the complex behaviour of Q2 as a result of two transitions that spectrally overlap, as indicated in the schematic potential diagram in Figure 18. One of the transitions is presumably related to an electron pocket at the interface to the GaN buffer layer, just as in sample A, while the additional transition is suggested to be due to a contribution of the next QW (Figure 18). Both transitions would obviously be downshifted with respect to Q1, due to the band bending. Unfortunately no PLE data could be obtained for this sample, since the p-layer on top absorbed the excitation light sufficiently to lower the signal below the detection limit in that experiment.

4.2.2 Time-resolved photoluminescence

The PL transient data at 2 K are shown in Figure 19. The short time decay for Q1 is about 3.5 ns, consistent with expectations for an exciton in a 3 nm wide QW. The Q2 peak has a longer decay time in Figure 19, about 12 ns. This would be expected for the tunneling transition across the narrow barrier in sample B, but also consistent with a QW exciton in the second QW, if the electric field is less screened due to a lower electron filling in that QW (Figure 18). A set of time resolved spectra for sample B are shown in Figure 20, together with the time integrated spectrum, for zero bias condition. Clearly there is an overlap of transitions in the spectral range of Q2, as evidenced also in the cw PL spectra discussed above. The different decay times of the spectral components make the time-integrated spectrum considerably broadened, as compared to the cw spectra in Figure 16. Note that the data in Figure 20 corresponds to the high excitation limit in Figure 16.

5 Discussion

5.1 The exciton linewidth in InGaN MQWs

The samples studied in this work constitute a reference in the sense that phase separation with nm size islands of higher In concentration appears to be absent, i. e. the QW alloy material is essentially a random alloy. This may be related to the growth technique employed, where the entire MQW region was grown at a temperature about 800°C, without temperature cycling. In most previous work, phase separation has been reported [3]

https://doi.org/10.1557/S1092578300000338 Published online by Cambridge University Press

[8] [32], and sometimes convincingly demonstrated, in high-resolution TEM (HRTEM) experiments [9] [10]. In our case, the optical data should be discussed in terms of exciton recombination affected by the internal polarization induced electric field and the localization potentials caused by both interface roughness and alloy fluctuations. The PL linewidth can conveniently be explained in this framework.

The distribution of the excitonic transition energy in QWs in the presence of alloy disorder and interface roughness is described by a Gaussian function with a standard deviation

$$\sigma^2 = \sigma_{alloy}^2 + \sigma_{rough}^2 \quad (1)$$

The contribution of the alloy disorder to the excitonic broadening is given by [33]

$$\sigma_{alloy} = 0.41 \left| \frac{dE_g(x)}{dx} \right| \sqrt{x(1-x) V_c / V_{ex}} \quad (2)$$

where V_c is the volume of the primitive cell and $V_{ex} = 4\pi a_B^3/3$ is the exciton volume. The composition variation of the bandgap energy at 2K of $In_xGa_{1-x}N$ is [34]

$$E_g = 3.493 - 2.843x - 2.5x(1 - x) \quad (3)$$

which gives $|dE_g/dx| = 4.74$ eV at $x = 0.12$. Using the values $a_B = 30$ Å and $V_c = 24$ Å^3, σ_{alloy} is estimated to be 9 meV for the random $In_{0.12}Ga_{0.88}N$ alloy. In case localisation in small In clusters occurs [35], this process would cause additional broadening not included in this formalism. The broadening due to the interface roughness is more difficult to calculate because σ_{rough} is sensitive to the lateral size of the valleys and islands as well as to the correlation between the two interfaces of the QW. The quality of the interface strongly depends on the growth condition and it will be very sample dependent. In nitride QWs, an enhancement of the broadening is expected due to the presence of the internal electric field. The electric field will force the electron and the hole closer the two opposite interfaces and therefore the exciton will experience the effect of the roughness more strongly. In the simple case of an equal density of the valleys and islands with lateral dimensions of order of a_B, σ_{rough} is given by [36]

$$\sigma_{rough} = \left| \frac{dE_{ex}^{QW}}{dL_w} \right| \delta L_w \quad (4)$$

where $|dE_{ex}^{QW}/dL_w|$ is the variation of the exciton transition energy with the well width and δL_w is the standard deviation of the probability distribution of the effective well width. For $In_{0.12}Ga_{0.88}N$/GaN QW with $L_w = 35$ Å and the well thickness fluctuation of 1 ML ($\delta L_w = 2.6$ Å) Equation (4) yields $\sigma_{rough} \approx 8$ meV for a square QW (zero field) and $\sigma_{rough} \approx 30$ meV for a triangular QW with a field of 1.1 MV/cm as estimated above for the sample A. The actual σ_{rough} value in our samples is expected to be between these two values because the field in the wells is partially screened by the electrons from Si-doped barriers. The full width at half maximum of the emission peak, FWHM = $\sigma(8\ln 2)^{1/2}$, is found to be 28 meV for a completely screened field and 74 meV for a field of 1.1 MV/cm. The experimentally obtained linewidth of 35-42 meV corresponds to a field of 0.5-0.6 MV/cm.

5.2 The lower energy peaks in photoluminescence

The presence of lower energy peaks in the PL spectra has previously been observed by many authors. One explanation for the lower energy peak observed has been the connection with the phase separation problem in the samples studied [3]. In other cases a lower energy peak has been observed in the near bandgap region, but has been related to dopants [37]. There is clearly a strong difference observed between optical spectra of MQW samples of similar In content in the active regions, but grown by a different MOVPE procedure in different laboratories. In our case the PLE data for sample A strongly suggest that the origin of a lower energy PL peak Q2 is an electron pocket at the interface to the GaN buffer layer, produced by the strong band bending near the surface of the MQW structure, which was grown without a cap layer. The spatially indirect transitions of this kind are very commonly observed in many heterojunction systems, such as AlGaAs/GaAs [38] and SiGe/Si [39], where the properties of the corresponding two-dimensional electron gas (2DEG) systems were studied in great detail. In this work we have not made any detailed studies of the 2DEG properties of Q2, however.

We point out that prerequisite for observation of the Q2 peak is that there is a potential step between the QW barrier material and the n-GaN buffer layer, so that the electrons can be localized at that interface. Consequently, in the cases the QW barriers are GaN and not InGaN, such a Q2 peak would be expected. Highly n-doped barriers are needed to obtain a strong potential

https://doi.org/10.1557/S1092578300000338 Published online by Cambridge University Press

gradient across the MQW part, localizing electrons at the barrier-buffer interface. Also, in cases when the MQW structure is not present at the surface, but buried under a top cover layer of GaN much thicker than the MQW dimension, the potential gradient across the MQW will be small, and the effect reported here will not be observed. These requirements explain why in most cases in the literature the Q2 peak was not reported.

5.3 Discussion on the MQW spectra in the presence of a strong potential gradient

The above data clearly show the presence of a strong potential gradient already for the region close to the GaN buffer layer. Such a gradient is indeed expected due to the uncompensated polarization charges at the top surface of the structure in sample A, combined with the presence of electrically active surface states [12] [14] [15] [16] [17] [18] [40] [41] [42]. In fact the only way a flat band condition could be realized in an MQW structure like in sample A would be the presence of an extremely high surface donor density at the conduction band edge, which is not very likely. Referring to our experimental data for sample A a strong gradient is necessary to leave the transition Q2 at lower photon energy than Q1 (Figure 4). The potential gradient clearly will be much larger close to the surface. The extent of the depletion region is expected to be very similar to the total MQW region in this particular case of a donor doping in the barriers in the order 5×10^{18} cm^{-3}. [41]. The observed Q1 transition is here interpreted as the excitonic PL from the lowest QW. This is at first sight surprising, since the excitation intensity is at least a factor 5 higher for the QW closest to the surface. However, the 3 QWs are positioned in very different depletion fields, which are superimposed on, and directed opposite to the internal polarization fields, dominated by the piezoelectric polarization charges [42]. The fields are both of the order 1 MV/cm, i. e. quite large. The depletion field may be estimated from the simple expression $F_d = F_{max}$ ($w - x$), where w is the depletion width and x is the distance from the surface. F_{max} at the outer surface is estimated from the simple expression $F_{max} = eN_d/\varepsilon_0\varepsilon$, giving a value about 2 MV/cm. (The uncertainty in this value mainly derives from incomplete knowledge of the number and charge status of the surface states at the outer surface, which give rise to a charge superimposed on the fixed surface spontaneous polarization charge.) F_d is expected to dominate the electric field across the two outer QWs. The magnitude of the internal field is still not well known; most experimental data indicate lower values of the field as compared to the theoretical estimates (about 1.1 MV/cm), i. e. well below 1 MV/cm in our case [43]. Since the total field across the QW is much higher for the near surface QWs, of the order >1 MV/cm for the doping used in this sample, their oscillator strength is expected to be strongly reduced [18]. The PL spectra of the two outer QWs would then be noticeably redshifted [18] [41], with an amount comparable to or larger than the 40 meV linewidth observed for the Q1 transition at lowest excitation intensity [18]. Since no trace is observed of additional QW spectra besides the Q1 line, we must conclude that only the lowest QW, i. e. the one closest to the GaN buffer layer, is radiative in sample A.

One possible explanation would be that the confinement of photo-excited carriers in the two outer QWs is insufficient in the high field region, in this case no PL can be observed. It is sufficient that one type of carrier in the QWs is unstable to cause quenching of the corresponding PL. Early theoretical estimates of the band offsets in InGaN/GaN interfaces are in line with a rather small valence band offset [44], so that the holes would be most unstable. More recent theoretical predictions give a different result for the relative size of the band offsets in the InGaN/GaN system, however [35]. Bellaiche et al predict a similar magnitude of the band offset for electrons and holes for In compositions relevant to our samples [35]. In that case confinement of photo-excited holes should be possible and the question arises whether perhaps instead the electrons in the high field QWs are not confined. Considering the strong band bending in the region of the two outer QWs, the width of the triangular barriers at the energy position of the electron ground state of the QW is below 1 nm, which would allow rather fast tunneling of electrons out of the QW, in particular if the InGaN barrier material is slightly defective, allowing point defect assisted tunneling. No PL would be observed if the tunneling time were smaller than the radiative lifetime of the QW, which is a few ns at low T. We tentatively conclude that the electrons easily become unstable in a strong depletion field as is present in sample A. This condition would apply to the two outermost QWs, while the third QW further away from the surface experiences a much lower depletion field, and is consequently optically active.

A similar situation seems to occur in sample B, where a similarly strong depletion field is caused by the p-n-junction. The 5 QWs are expected to be just inside the extent of the depletion region at zero bias, due to the strong n-doping in the barriers [41]. The QW closest to the GaN buffer is presumably in a very low depletion field and should have some electron filling; hence it is strongly radiative. The next one is more inside the depletion region, but the depletion field is presumably not strong enough to cause substantial carrier leakage out of the QW, hence this QW gives rise to a PL line

https://doi.org/10.1557/S1092578300000338 Published online by Cambridge University Press

downshifted in energy compared to the first QW, due to a smaller electron filling. The other 3 QWs are not seen at zero bias, but observed in PL at forward bias and in electroluminescence, when the depletion field is quenched to a large extent, and no carrier leakage occurs (Figure 21). The data under bias are described in more detail elsewhere [20] [45].

6 Summary

In summary we report a detailed optical study of InGaN MQW structures grown at a fixed temperature of 800°C. The QW emission is identified as being of excitonic nature, strongly influenced by localization in the low temperature range (< 150 K) in spite of the presence of carriers supplied by the doped barriers. The localization is mainly responsible for the rather strong LO-phonon coupling observed in these samples. The PL linewidth of about 35-40 meV at low T is conveniently explained as dominated by the interface roughness, with a small contribution from alloy broadening. A lower energy PL peak is not due to phase separation, rather is it connected to an electron pocket at the interface to the underlying thick GaN buffer layer. The absence of phase separation is consistent with TEM data on a series of similar samples. Our data also show a drastic influence of the surface depletion field on the photoluminescence of doped InGaN/GaN MQW structures. For the samples studied in this work we conclude that only the QW in the lowest field closest to the buffer layer seems to be active in the PL experiment, the other QWs closer to the surface apparently cannot hold the carriers in the strong depletion field. For an undoped MQW system the depletion field would be much smaller and cover a much wider region, which should give a different result.

REFERENCES

[1] Shuji Nakamura, Gerhard Fasol, *The Blue Laser Diode - GaN based Light Emitters and Lasers* , (Springer-Verlag, Heidelberg, 1997), .

[2] S. F. Chichibu, A. Shikanai, T. Deguchi, A. Setoguchi, R. Nakai, H. Nakanishi, K. Wada, S. P. DenBaars, T. Sota, S. Nakamura, *Jpn. J. Appl. Phys.* ***39***, 2417 (2000).

[3] Y. Narukawa, Y. Kawakami, S. Fujita, S. Fujita, S. Nakamura, *Phys. Rev. B* ***55***, R1938 (1997).

[4] T. Sugahara, S. Sakai, M. Lachab, R. S. Q. Fareed, S. Tottori, T. Wang, *Phys. Stat. Sol. B* ***216***, 273 (1999).

[5] B. Monemar, J. P. Bergman, J. Dalfors, G. Pozina, B.E. Sernelius, P.O. Holtz, H. Amano, I. Akasaki, *MRS Internet J. Nitride Semicond. Res.* ***4***, 16 (1999).

[6] P. Lefebvre, A. Morel, M. Gallart, T. Taliercio, J. Allegre, B. Gil, H. Mathieu, B. Damilano, N. Grandjean, J. Massies, *Appl. Phys. Lett.* ***78***, 1252 (2001).

[7] P. Waltereit, O. Brandt, J. Ringling, K. H. Ploog, *Phys. Rev. B* ***64***, 245305 (2001).

[8] K. P. O'Donnell, R. W. Martin, P. G. Middleton, *Phys. Rev. Lett.* ***82***, 237 (1999).

[9] F. A. Ponce, D. Cherns, W. Goetz, R. S. Kern, *Mater. Res. Soc. Symp. Proc.* ***482***, 453 (1998).

[10] P. Ruterana, in "Low Dimensional Nitride Semiconductors", edited by B. Gil, (Oxford University Press, Oxford, 2002), p. 151

[11] B. Monemar, P. P. Paskov, G. Pozina, T. Paskova, J. P. Bergman, M. Iwaya, S. Nitta, H. Amano, I. Akasaki, *Phys. Stat. Sol. B* ***228***, 157 (2001).

[12] B. Monemar, G. Pozina, *Prog. Quantum Electron.* ***24***, 239 (2000).

[13] C Wetzel, T Takeuchi, H Amano, I Akasaki, *Jpn. J. Appl. Phys.* ***38***, L163-5 (1999).

[14] O. Ambacher, J. Majewski, C. Miskys, A. Link, M. Hermann, M. Eickhoff, M. Stutzmann, F. Bernardini, V. Fiorentini, V. Tilak, B. Schaff, L. F. Eastman, *J. Phys. C* ***14***, 3399 (2002).

[15] F. Bernadini, V. Fiorentini, D. Vanderbilt, *Phys. Rev. B* ***56***, R10024 (1997).

[16] F. Bernadini, V. Fiorentini, D. Vanderbilt, *Phys. Rev. B* ***63***, 193201 (2001).

[17] F. Bernadini, V. Fiorentini, *Phys. Rev. B* ***64***, 085207 (2001).

[18] V. Fiorentini, F. Bernadini, F. Della Sala, A. Di Carlo, P. Lugli, *Phys. Rev. B* ***60***, 8849 (1999).

[19] A. Reznitsky, A. Klochikhin, S. Permogorov, L. Tenishew, W. Lundin, A. Usikov, M. Schmidt, C. Klingshirn, unpublished.

[20] B. Monemar, P. P. Paskov, G. Pozina, J. P. Bergman, T. Paskova, M. Iwaya, S. Kamiyama, H. Amano, I. Akasaki, *Phys. Stat. Sol. A* ***192***, 21 (2002).

[21] H. Amano, N. Sawaki, I. Akasaki , Y. Toyoda , *Appl. Phys. Lett.* ***48***, 353-355 (1986).

[22] V. Darakchieva, T. Paskova, P. P. Paskov, B. Monemar, N. Askenov, M. Schubert, unpublished.

[23] W. Paszkowicz, *Powd. Diff.* ***14***, 258 (1999).

[24] A. Polian , M. Grimsditch , I. Grzegory , *J. Appl. Phys.* ***79***, 3343-3344 (1996).

[25] AF Wright, *J. Appl. Phys.* ***82***, 2833-2839 (1997).

[26] A. S. Barker, M. Ilegems, *Phys. Rev. B* ***7***, 743 (1973).

[27] F. Bernadini, V. Fiorentini, *Phys. Rev. Lett.* ***79***, 3958 (1997).

[28] B. Monemar, P. P. Paskov, T. Paskova, J. P. Bergman, G. Pozina, W. M. Chen, P. N. Hai, I. A. Buyanova, H. Amano, I. Akasaki, *Mater. Sci. Eng. B* ***93***, 112 (2002).

[29] P. P. Paskov, P. O. Holtz, B. Monemar, S. Mamiyama, M. Iwaya, H. Amano, I. Akasaki, unpublished.

[30] Marco Buongiorno Nardelli, Krzysztof Rapcewicz, J. Bernholc, *Appl. Phys. Lett.* ***71***, 3135 (1997).

[31] J. Martinez-Pastor, A. Vinattieri, I. Carraresi, M. Collocci, P. Roussignol, B. Weimann, *Phys. Rev. B* ***47***, 10456 (1993).

[32] Yu. G. Musikhin, D. Gerthsen, D. A. Bedarev, N . A. Bert, W. V. Lundin, A. F. Tsatsulnikov, A. V. Sakharov, A. S. Usikov, Zh. I. Alferov, I. L. Krestnikov, N. N. Ledentsov, A. Hoffmann, D. Bimberg, *Appl. Phys. Lett.* ***80***, 2099 (2002).

[33] G. Coli, K. K. Bajaj, J. Li, J. Y. Lin, H. X. Xiang, *Appl. Phys. Lett.* ***80***, 2907 (2002).

[34] V. Yu. Davydov, A. A. Klochikhin, V. V. Emtsev, S. V. Ivanov, V. V. Vekshin, F. Bechstedt, J. Furthmuller, H.

https://doi.org/10.1557/S1092578300000338 Published online by Cambridge University Press

Harima, A. V. Mudryi, A. Hashimoto, A. Yamamoto, J. Aderhold, J. Graul, E. E. Haller, *Phys. Stat. Sol. B* ***230***, R4 (2002).

[35] L. Bellaiche, T. Mattila, L. W. Wang, S. H. Wei, A. Zunger, *Appl. Phys. Lett.* ***74***, 1842 (1999).

[36] J. Singh, K. K. Bajaj, *J. Appl. Phys.* ***57***, 5433 (1985).

[37] T. Wang, H. Saeki, J. Bai, T. Shirahama, M. Lachab, S. Sakai, P. Eliseev, *Appl. Phys. Lett.* ***76***, 1737 (2000).

[38] Q. X. Zhao, Y. Fu, P. O. Holtz, B. Monemar, J. P. Bergman, K. A. Zhao, M. Sundaram, J. L. Merz, A. C. Gossard, *Phys. Rev. B* ***43***, 5035 (1991).

[39] I. A. Buyanova, W. M. Chen, A. Henry, W. X. Ni, G. V. Hansson, B. Monemar, *Phys. Rev. B* ***53***, 9587 (1996).

[40] G. Pozina, J. P. Bergman, B. Monemar, M. Iwaya, S. Nitta, H. Amano, I. Akasaki, *Appl. Phys. Lett.* ***77***, 1638 (2000).

[41] O. Mayrock, H. J. Wunsche, F. Henneberger, *Phys. Rev. B* ***62***, 16870 (2000).

[42] R. Lantier, A. Rizzi, H. Luth, O. Mayrock, H. J. Wunsche, F. Henneberger, M. Lomascolo, R. Cingolani, "Optical emission from surface and buried AlGaN/GaN MQWs grown by MBE on 6H-SiC", Proc. Int. Workshop on Nitride Semiconductors, IPAP Conference Series 1 (Tokyo), p. 166

[43] C. Wetzel, T. Takeuchi, H. Amano, I. Akasaki, *Phys. Rev. B* ***61***, 2159 (2000).

[44] CG Van der Walle, J Neugebauer, *Appl. Phys. Lett.* ***70***, 2577-2579 (1997).

[45] B. Monemar, P. P. Paskov, H. Haratizadeh, P. O. Holtz, J. P. Bergman, S. Kamiyama, M. Iwaya, H. Amano, I. Akasaki, unpublished.

FIGURES

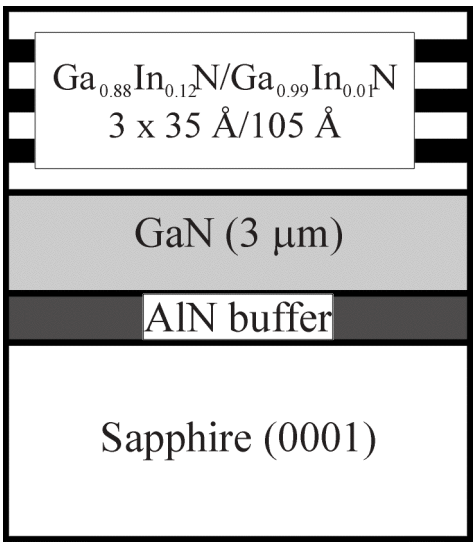

Figure 1a. Schematic picture of the structure of sample A.

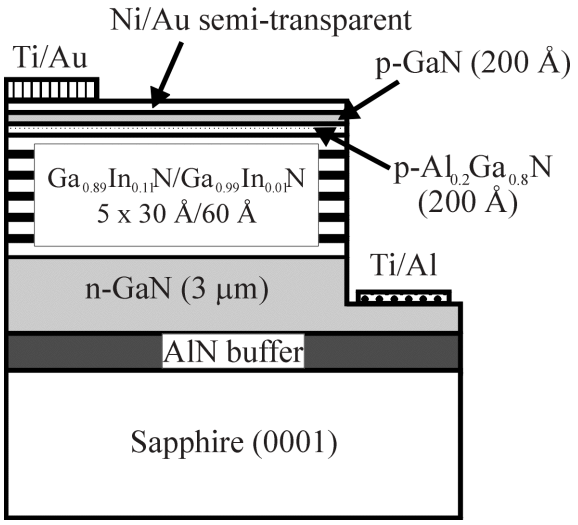

Figure 1b. Schematic picture of the structure of sample B.

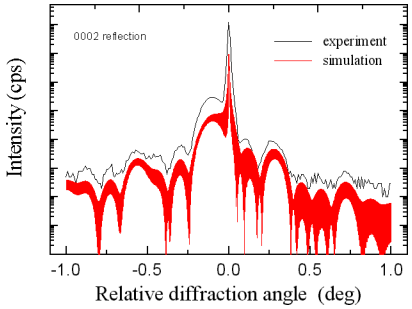

Figure 2. Measured (black thin line) and simulated (thick red line) 0002 profiles of sample A.

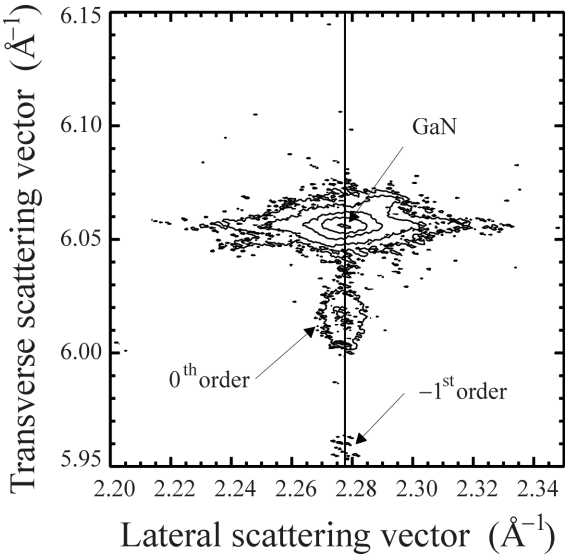

Figure 3. Asymmetric 10-15 reciprocal space mapping of sample A. The vertical line marks the direction of fully strained growth of the MQW structure.

https://doi.org/10.1557/S1092578300000338 Published online by Cambridge University Press

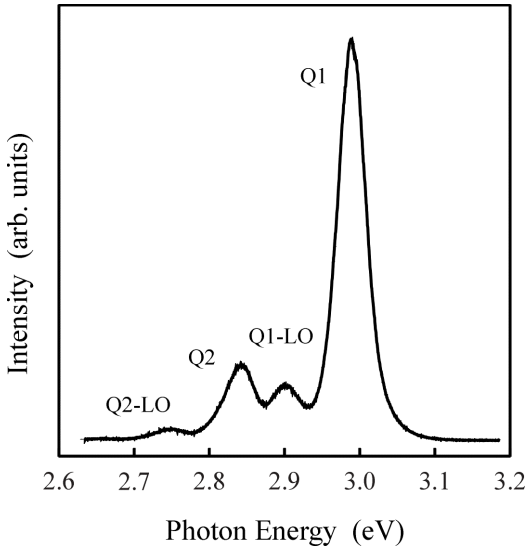

Figure 4. Photoluminescence spectra of sample A at 2 K and low cw excitation intensity.

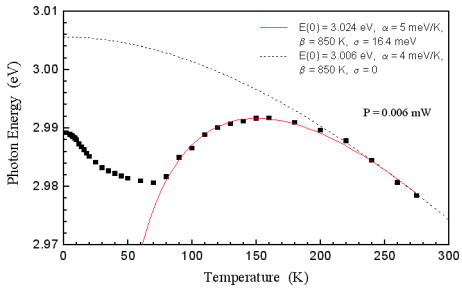

Figure 5a. Temperature dependence of the main emission peak Q1 of sample A at excitation power P = 0.006 mW. Experimental data are fitted with the expression $E = E(0) - \alpha T^2/(T + \beta) - \sigma^2/kT$.

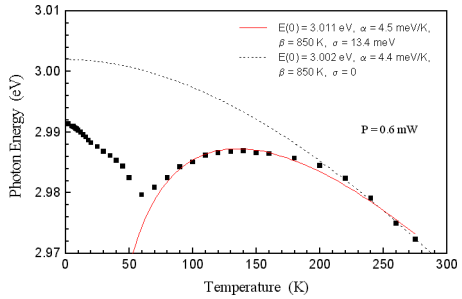

Figure 5b. Same as Figure 5a but at excitation power P = 0.6 mW.

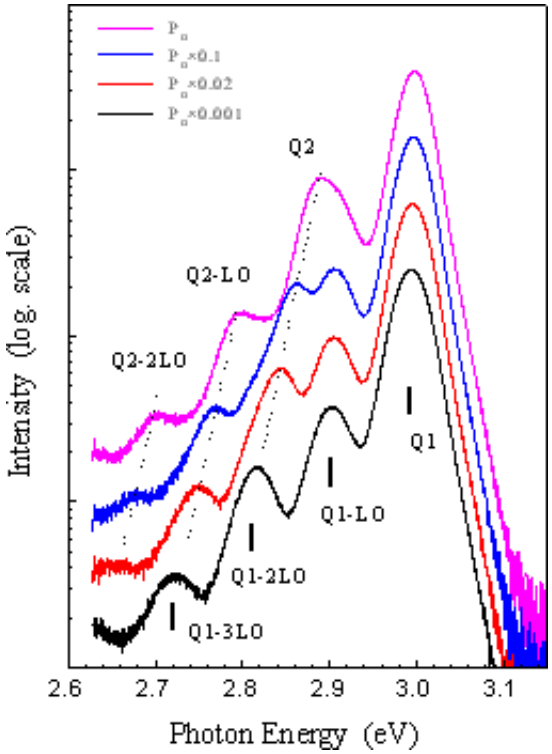

Figure 6. Low-temperature PL spectra of sample A at different excitation powers. The spectra are shifted for clarity. The dashed lines are guide to the eyes.

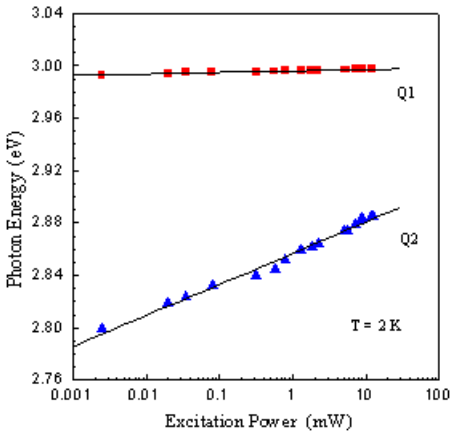

Figure 7. Energy position of the Q1 and Q2 emission peaks as a function of the excitation power. The lines are guide to the eyes.

https://doi.org/10.1557/S1092578300000338 Published online by Cambridge University Press

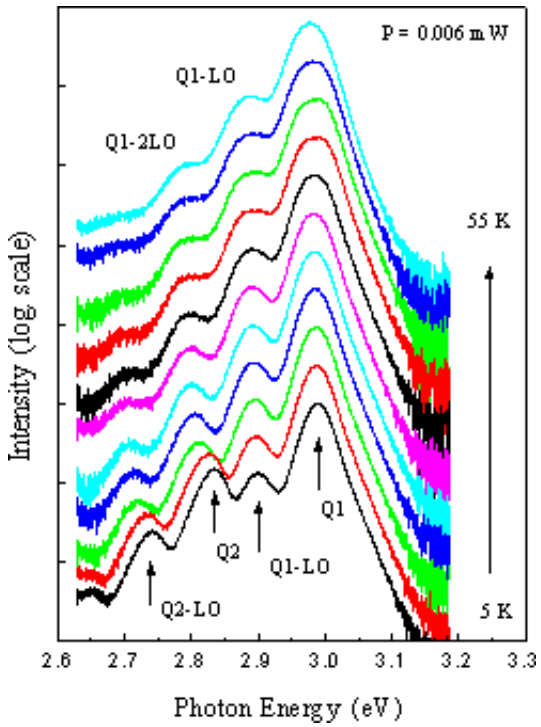

Figure 8a. PL spectra of sample A at different temperatures between 5 K and 55 K.

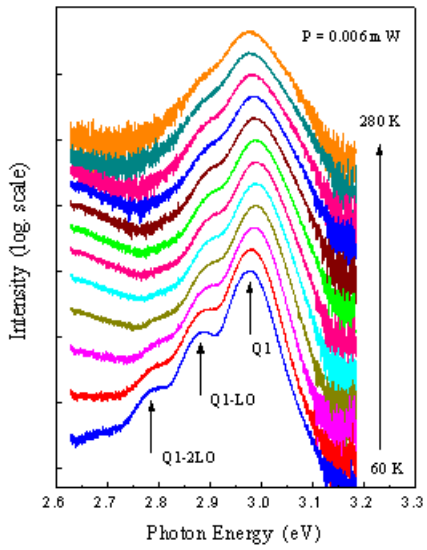

Figure 8b. PL spectra of sample A at temperatures above 60 K.

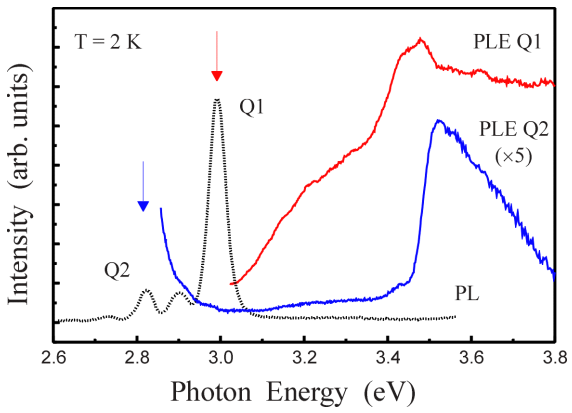

Figure 9. Photoluminescence excitation spectra of sample A.

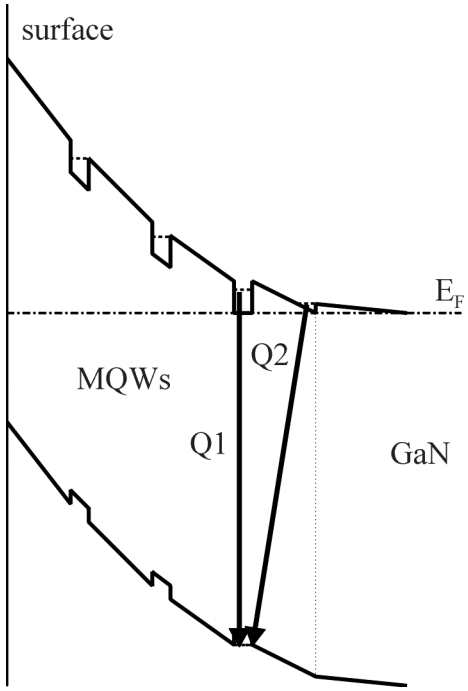

Figure 10. Sketch of the potential variation across the MQW region for sample A.

MRS Internet J. Nitride Semicond. Res. 7, 7 (2002).

https://doi.org/10.1557/S1092578300000338 Published online by Cambridge University Press

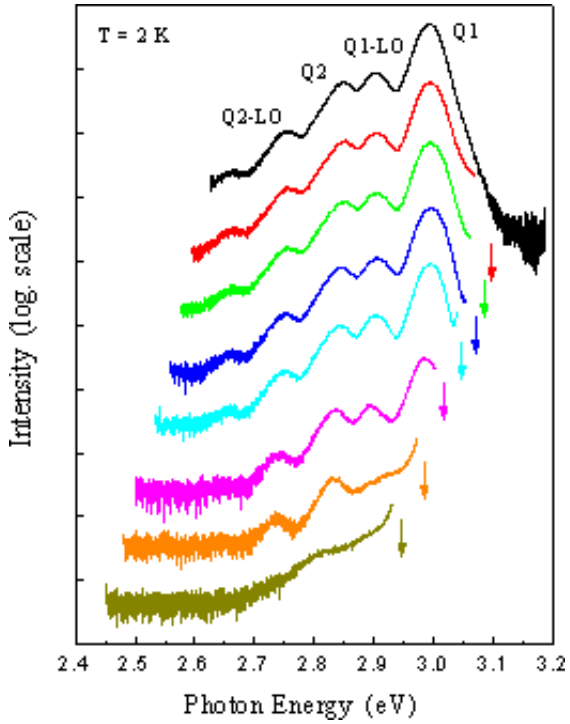

Figure 11. Low temperature PL spectra of the sample A at different excitation energies below the barrier bandgap. The arrows indicate the excitation energies.

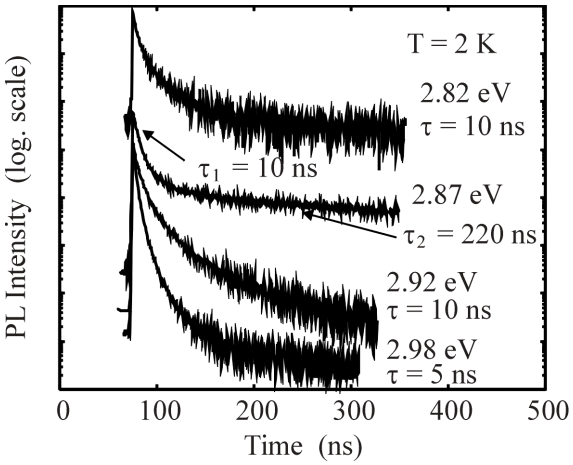

Figure 12. Low temperature PL transients of sample A measured for selected photon energies.

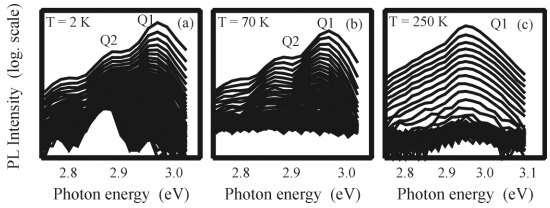

Figure 13. Time-resolved spectra of sample A measured at different temperatures: 2 K (a), 70 K (b) and 250 K (c). The time interval between each spectrum is 1.9 ns.

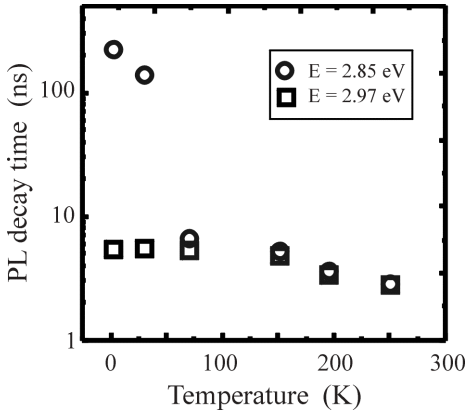

Figure 14. Temperature dependence of the photoluminescence decay time of Q1 and Q2 transitions.

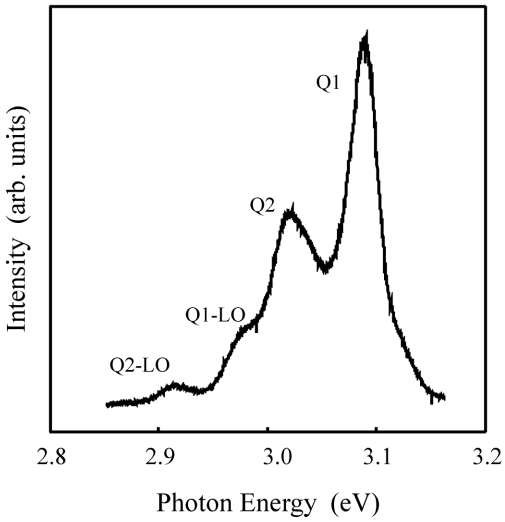

Figure 15. PL spectra of sample B at T = 2K.

https://doi.org/10.1557/S1092578300000338 Published online by Cambridge University Press

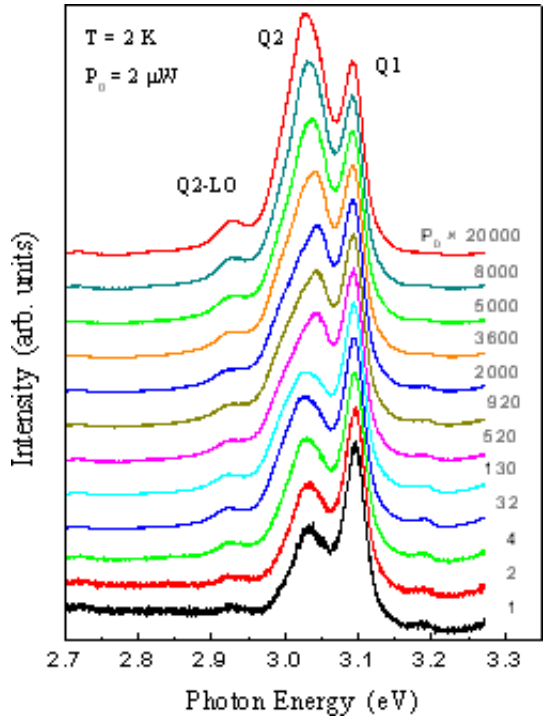

Figure 16. PL spectra of sample B at different excitation intensities. The spectra are normalized and shifted for clarity.

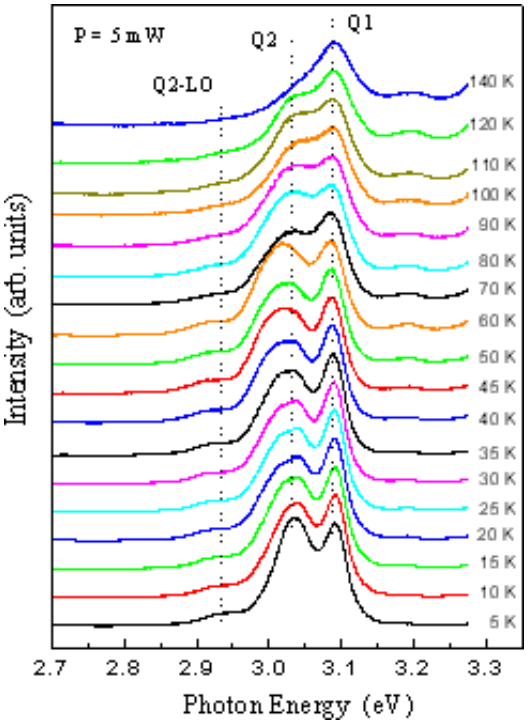

Figure 17b. Temperature dependent PL spectra of sample B at high excitation intensity.

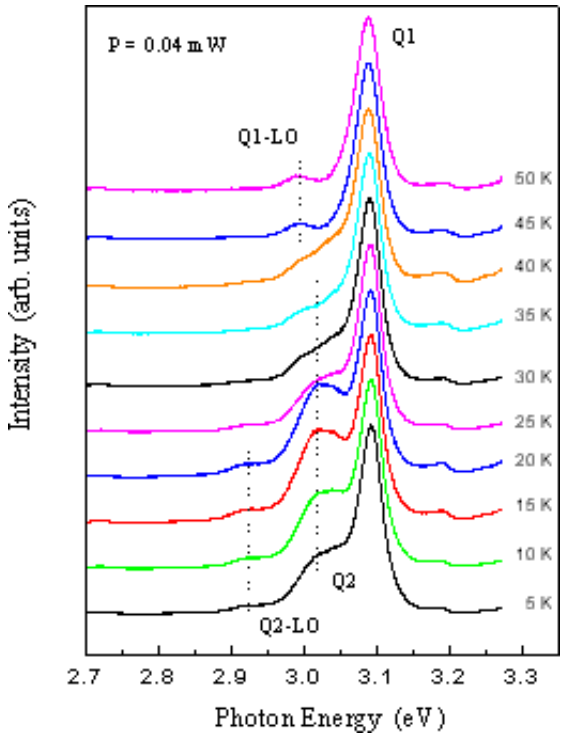

Figure 17a. Temperature dependent PL spectra of sample B at low excitation intensity.

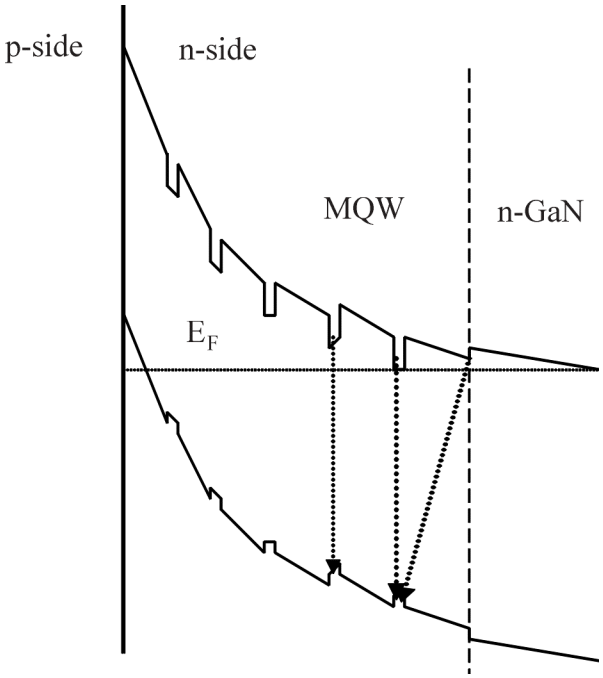

Figure 18. Sketch of the potential variation across the MQW region for sample A.

https://doi.org/10.1557/S1092578300000338 Published online by Cambridge University Press

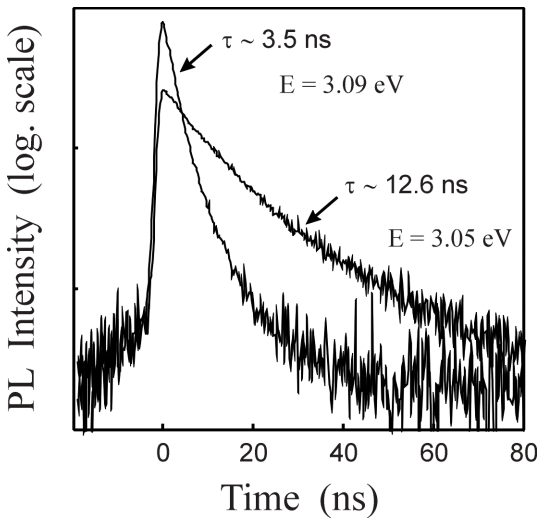

Figure 19. Photoluminescence transients for Q1 and Q2 transitions of sample B at T = 2 K.

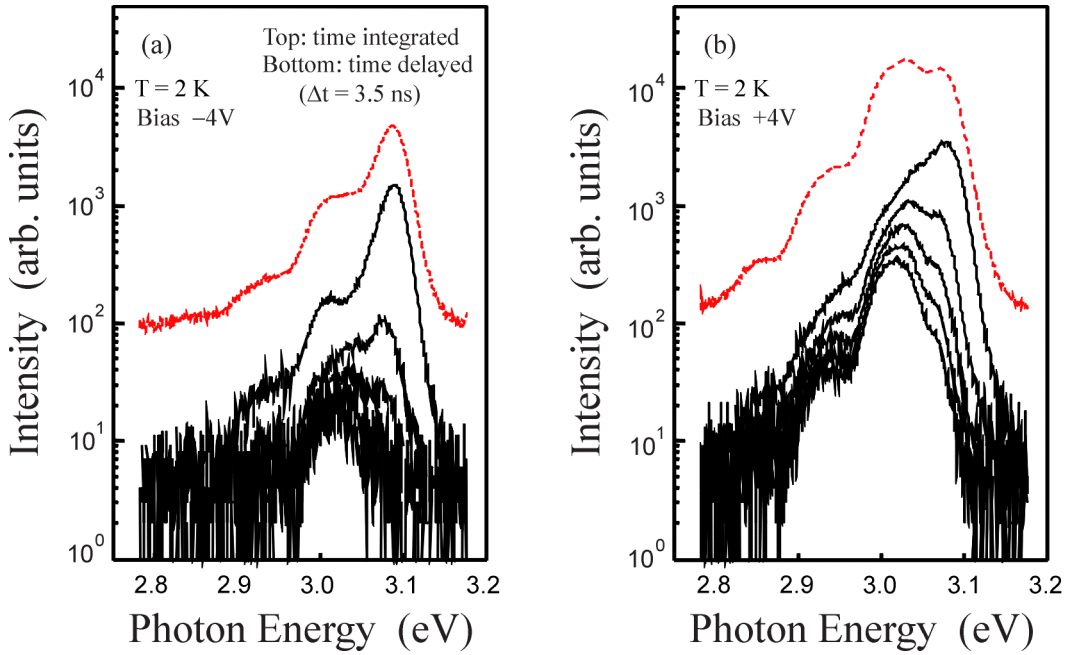

Figure 20. Time-resolved PL spectra for sample B with different external bias: (a) –4V and (b) +4V. The top spectrum is a time-integrated spectrum shown for comparison. The delay time between successive spectra is 3.5 ns.

https://doi.org/10.1557/S1092578300000338 Published online by Cambridge University Press

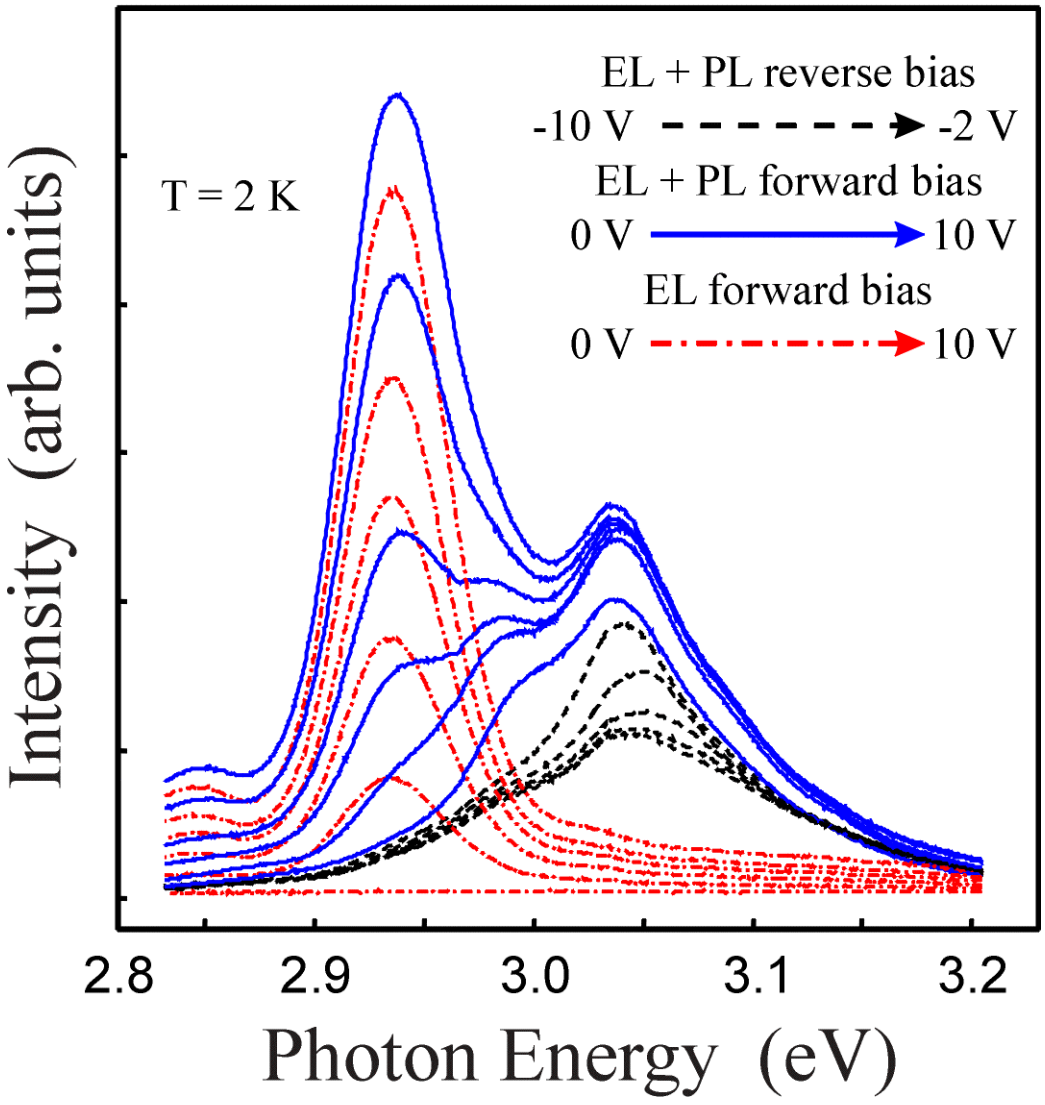

Figure 21. Photoluminescence (PL) and electroluminescence (EL) of sample B at different applied biases and T = 2 K. There is a series resistance in the electrical wires down to the sample in the cryostat, so the real bias over the sample is smaller by a factor two. The EL spectra are obtained without optical excitation with DC bias.

TABLES

Table 1. Table 1. Values of parameters used in estimation of the internal electric field.

	$In_{0.12}Ga_{0.88}N$ well	$In_{0.01}Ga_{0.99}N$ barrier
$(a–a_0)/a_0$	–0.0140	–0.0022
e_{33} (C/m^2)	0.76	0.73
e_{13} (C/m^2)	–0.50	–0.49
C_{13} (GPa)	104	106
C_{33} (GPa)	377	396
P_{pz} (C/m^2)	0.0174	0.0026
ε	10.8	10.3
E (V/m)	$–1.125\times10^8$	0.42×10^8

https://doi.org/10.1557/S1092578300000338 Published online by Cambridge University Press